Inorganic Chemistry

Article

pubs.acs.org/IC

A Six-Coordinate Ytterbium Complex Exhibiting Easy-Plane Anisotropy and Field-Induced Single-Ion Magnet Behavior

Jun-Liang Liu,[†,∥] Kang Yuan,[†,∥] Ji-Dong Leng,[†] Liviu Ungur,[‡] Wolfgang Wernsdorfer,*[,§] Fu-Sheng Guo,[†] Liviu F. Chibotaru,*[,‡] and Ming-Liang Tong*[,†]

[†]MOE Key Lab of Bioinorganic and Synthetic Chemistry, State Key Laboratory of Optoelectronic Materials and Technologies, School of Chemistry & Chemical Engineering, Sun Yat-Sen University, Guangzhou 510275, P. R. China

[‡]Division of Quantum and Physical Chemistry and INPAC—Institute of Nanoscale Physics and Chemistry, Celestijnenlaan 200F, Katholieke Universiteit Leuven, B-3001, Belgium

[§]Department of Chemistry and Biochemistry-0358, University of Institut Néel, CNRS & Université Joseph Fournier, BP 166, 25 avenue des Martyrs, 38042 Grenoble Cedex 9, France

Supporting Information

ABSTRACT: The field-induced blockage of magnetization behavior was first observed in an Yb^{III}-based molecule with a trigonally distorted octahedral coordination environment. Ab initio calculations and micro-SQUID measurements were performed to demonstrate the exhibition of easy-plane anisotropy, suggesting the investigated complex is the first pure lanthanide field-induced single-ion magnet (field-induced SIM) of this type. Furthermore, we found the relaxation time obeys a power law instead of an exponential law, indicating that the relaxation process should be involved a direct process rather than an Orbach process.

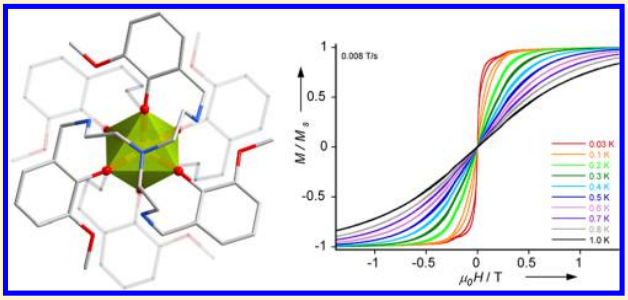

INTRODUCTION

In pursuit of the potential applications on ultrahigh-density memory, molecular spintronic devices, and quantum computing, molecule-based magnets with an energy barrier between the bistable ground states that slows the relaxation of the spin, known as single-molecule magnets (SMMs), have been recognized as highly promising candidates.[1,2] In addition to the transition-metal-cluster complexes with a high-spin ground state but a comparatively small anisotropy,[3] a class of SMMs containing just a single paramagnetic ion, which is called single-ion magnet (SIM), has attracted much attention in recent years.[4−12] In general, when the paramagnetic ion with spin−orbit coupled ground-state (J) is placed in a proper ligand-field (LF), the removal of $(2J + 1)$-fold degeneracy sublevels lowers the energy of the larger $\pm M_J$ doublets rather than the smaller ones, leading to an easy axis of the magnetization.[4] Moreover, for Kramers ions (odd electron count), since the $\pm M_J$ doublets cannot be broken in the absence of magnetic field due to time-reversal symmetry considerations,[2f,13] an easy-plane anisotropy with a smaller quantum number is also possible toward SIMs. Thus, both of the metallic species and the LF symmetry play crucially important roles.

Since Ishikawa first discovered the lanthanide phthalocyanine complexes exhibiting an extremely slow relaxation rate in 2003,[4] to date, a few SIMs or field-induced SIMs based on lanthanide,[4−9] actinide,[10,11] and transition metal[12] were continuously reported. Ishikawa et al.[5a] and Carretta et al.[6] demonstrated that the reduction or the matrix arrangements for $[Pc_2Tb^{III}]^-$ anion can significantly change the LF of the SIM. The slow relaxation behavior can be tuned by Long et al. and Murugesu and Richeson et al. via substituting the ligand of the trigonal pyramidal transition-metal complexes.[12b,e] For lanthanide SIMs, most of them are 8-coordinate with square-antiprism geometry (pseudo D_{4d}). Gao et al.[8] and Li and You et al.[9a] also showed that the different local symmetry leads to distinct magnetic dynamic behavior. Finding a new-type of SIM with a unique coordination environment makes chemists and physicist better understand the role of the symmetry of the LFs and the magnetic dynamics of the SIMs.

Herein, we report a 6-coordinate ytterbium(III) complex, $[Yb^{III}(\mathbf{H_3L})_2]Cl_3{\cdot}5CH_3OH{\cdot}2H_2O$ (Figure 1 and Table 1), where $\mathbf{H_3L}$ = tris(((2-hydroxy-3-methoxybenzyl)amino)ethyl)-amine. The ligand $\mathbf{H_3L}$ was produced from in situ condensation and reduction of *o*-vanillin, tris(2-aminoethy1)amine, and $NaBH_4$. Actually, an analog was first reported in 1993,[14a] but that of the counteranion is nitrate instead of chloride. The complex possesses a distorted octahedral geometry, which is the lowest coordination number so far as the pure lanthanide SIMs and field-induced SIMs.[4−12] To our knowledge, there is quite a small number of the reported Yb^{III}-based complexes behaving as SIMs or field-induced SIMs.[4b,7a] Ab initio

Received: May 27, 2012
Published: July 16, 2012

dx.doi.org/10.1021/ic301115b | Inorg. Chem. 2012, 51, 8538−8544

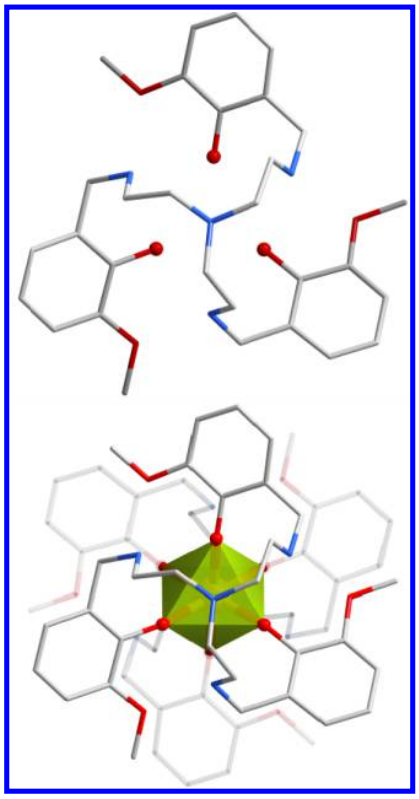

Figure 1. The in situ generated ligands $\mathbf{H_3L}$ (top) and the structure of the $[Yb^{III}(\mathbf{H_3L})_2]^{3+}$ cation (bottom). The Yb^{III} is highlighted as a green polyhedron. Orange, gray, red, and blue spheres represent Yb, C, O, and N atoms, respectively. Hydrogen atoms have been omitted for clarity.

Table 1. Crystal Data and Structure Refinements

chemical formula	$C_{65}H_{108}Cl_3N_8O_{19}Yb$
formula mass	1584.98
crystal system	monoclinic
a/Å	25.760(5)
b/Å	15.080(5)
c/Å	21.271(2)
β/°	114.844(10)
unit cell volume/Å^3	7498(3)
temperature/K	293(2)
space group	$C2/c$
no. of formula units per unit cell, Z	4
radiation type	Mo Kα
absorption coefficient, μ/mm^{-1}	1.426
no. of reflections measured	17508
no. of independent reflections	7060
R_{int}	0.0858
final R_1 values[a] ($I > 2\sigma(I)$)	0.0784
final $wR(F^2)$ values[b] (all data)	0.1703
goodness of fit on F^2	1.051

[a] $R_1 = \sum||F_o| - |F_c||/\sum|F_o|$. [b] $wR_2 = [\sum w(F_o^2 - F_c^2)^2/\sum w(F_o^2)^2]^{1/2}$.

calculations and micro-SQUIDS measurements were performed, indicating the complex exhibits easy-plane anisotropy. In addition, the analysis of the relaxation mechanism implied the spin−lattice relaxation should be involved in a direct process.

EXPERIMENTAL SECTION

Materials and General Procedures. All of the chemicals were obtained from commercial sources and used without further purification. The C, H, and N microanalyses were carried out with an Elementar Vario-EL CHNS elemental analyzer. The FT-IR spectra were recorded from KBr pellets in the range of 4000−400 cm^{-1} with a Bruker-EQUINOX 55 FT-IR spectrometer. The powder X-ray diffraction (pXRD) intensities for polycrystalline samples were measured at room temperature on a Bruker D8 Advance diffratometer (Cu Kα, λ = 1.54056 Å) by scanning over the range of 5−60° with a step of 0.2 °/s. The calculated patterns were generated with Mercury.

Synthesis. *$[Yb^{III}(H_3L)_2]Cl_3{\cdot}5CH_3OH{\cdot}2H_2O$ (1).* A mixture of *o*-vanillin (46 mg, 0.3 mmol) and tris(2-aminoethy1)amine (15 mg, 0.1 mmol) in methanol (15 mL) was stirred for 10 min, yielding an orange solution. $NaBH_4$ (14 mg, 0.4 mmol) was added to the solution. Five minutes later, the orange color disappeared. Then, $YbCl_3{\cdot}6H_2O$ (39 mg, 0.1 mmol) was added, and the colorless solution was stirred for an additional 2 h. After that, the solution was filtered, and the filtrate was left standing at room temperature for evaporation. Colorless crystals available for single crystal diffraction were obtained a few days later. Colorless crystals were obtained from the filtration in ∼20% yield based on *o*-vanillin. Anal. Calc. (%): N, 7.07; C, 49.26; H, 6.87; Found (%): N, 7.09; C, 49.13; H, 6.83. IR data (KBr, cm^{-1}): 3402 m, 2999 m, 2951 m, 2832 m, 1570 m, 1476 vs, 1357 m, 1278 vs, 1251 vs, 1078s, 848 m, 741 s.

X-ray Structure Determination. The intensity data was recorded on a Rigaku R-AXIS SPIDE IP system with Mo Kα radiation. The structure was solved by direct methods, and all nonhydrogen atoms were refined anisotropically by least-squares on F^2 using the SHELXTL program. Hydrogen atoms on organic ligands were generated by the riding mode (G. M. Sheldrick, SHELXTL97, program for crystal structure refinement, University of Göttingen, Germany, 1997).[15b] The disordered water and methanol molecules could not be modeled properly; thus, the program SQUEEZE,[15a] a part of the PLATON package of crystallographic software, was used to calculate the solvent disorder area and remove its contribution to the overall intensity data. CCDC-872761 contains the supplementary crystallographic data for this paper. These data can be obtained free of charge via www.ccdc.cam.ac.uk/conts/retrieving.html (or from the Cambridge Crystallographic Data Centre, 12 Union Road, Cambridge CB21EZ, UK; fax: (+44)1223-336-033; deposit@ccdc.cam.ac.uk).

Magnetic Measurements. Magnetic susceptibility measurements were performed using a Quantum Design MPMS XL-7 SQUID magnetometer. Diamagnetism was estimated from Pascal constants.

Micro-SQUID Measurements. Magnetization measurements on oriented single crystals were carried out with an array of micro-SQUIDs.

Computational Methodology. All calculations were done with MOLCAS 7.6 and are of CASSCF/RASSI/SINGLE_ANISO type.

RESULTS AND DISCUSSION

Structural Analysis. The single X-ray crystallography reveals that the complex crystallizes in the $C2/c$ space group. In the complex, the three "arms" of $\mathbf{H_3L}$ form a left-handed screw on one side and a right-handed screw on the other side. Yb^{III} is coordinated by six oxygen atoms which come from the phenoxy group of the ligands and possesses a trigonally distorted octahedron with *fac*-term (Figures 1 and S1, Supporting Information). Strictly speaking, the $[Yb^{III}(\mathbf{H_3L})_2]^{3+}$ cations have C_i rather than the ideal O_h local symmetry. The Yb−O distances vary from 2.224(6) Å to 2.235(8) Å, and Σ = 57.2°,[16c,d] which indicates the tiny deviation from the ideal octahedron. The continuous shape measurements (CShM) values ($S_{(Oh)}$ = 0.35 and $S_{(itp)}$ = 15.37) calculating by program SHAPE 2.0 assign the coordination geometry to the elongated trigonal antiprism (pseudo S_6 or pseudo D_{3d} local symme-

dx.doi.org/10.1021/ic301115b | Inorg. Chem. 2012, 51, 8538−8544

try).[16a,b] For simplicity, an ascend-of-symmetry operation, $C_i \rightarrow S_6 \rightarrow D_{3d} \rightarrow O_h$, can be used to describe the local symmetry.

Adjacent $[Yb^{III}(\mathbf{H_3L})_2]^{3+}$ cations are separated from each other in quite a long distance of 12.8 Å, suggesting the intermolecular magnetic interactions between the 6-coordinate Yb^{III} can be omitted. It is worth mentioning that the protons should attach to the oxygen atoms (phenol type) instead of the nitrogen atoms (secondary ammonium type), because (a) in methanol the acid dissociation constant (pK_a) of phenols (phenol: 14.33; salicylaldehyde: 12.82) are larger than that of the ammoniums (dimethylamine: 11.20; triethylamine: 10.78).[14b] Therefore, the phenol type is a more thermodynamic stable entity in methanol. (b) The IR spectra showed that the two new peaks which were related to the stretching vibration and the bending vibration of the secondary ammoniums ($[RR'NH_2]^+$) are absent for the Yb^{III} complex and its alkali-treated sample, while the peaks occur for the acid-treated one (Figure 2), suggesting the absence of secondary ammonium in the Yb^{III} complex.

Magnetic Properties. The temperature dependence of the $\chi_M T$ product is shown in Figure 3. The value of $\chi_M T$ is 2.43 cm^3 mol^{-1} K at 300 K, slightly smaller than the expected value of 2.57 cm^3 mol^{-1} K (Yb^{III}, $^2F_{7/2}$, $S = {}^1/_2$, $L = 3$, $J = {}^7/_2$, $g_J = {}^8/_7$).[17a−c] On cooling, the $\chi_M T$ value gradually decreases to 0.70 cm^3 mol^{-1} K at 2 K, which is mostly attributed to the progressive thermal depopulation of the excited-state Stark sublevels due to the crystal-field effects of Yb^{III}. The field dependence of magnetization (Figure 3, bottom) rises slowly before reaching 1.42 $N\beta$ at 2.0 K, as a result of the magnetic anisotropy.

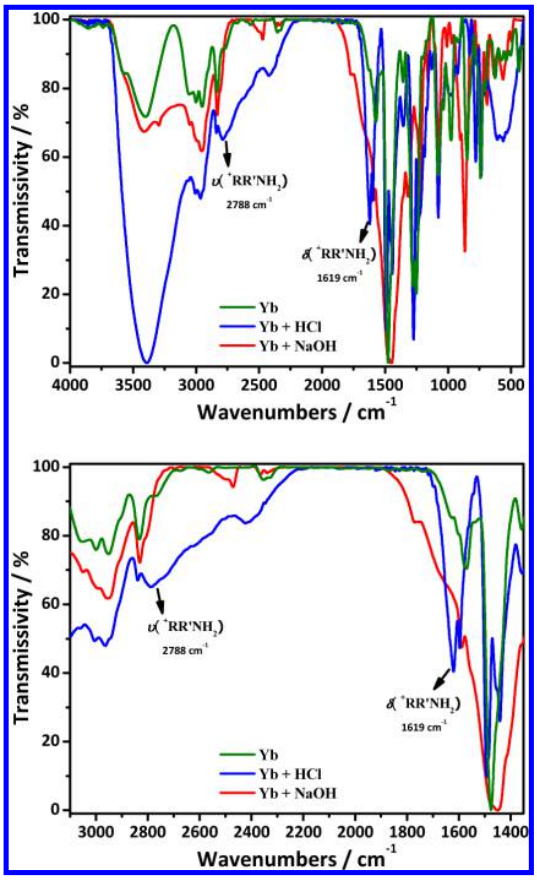

Figure 2. FT-IR spectra of the Yb^{III} complex and its acid-treated and alkali-treated ones. Top: 400−4000 cm^{-1}. Bottom: 1350−3100 cm^{-1}. Two new peaks (the stretching vibration and the bending vibration) which are related to the secondary ammonium ($[RR'NH_2]^+$) occur for the acid-treated sample, while the peaks are absent for the alkali-treated sample and the Yb^{III} complex, indicating the Yb^{III} complex should be the phenol type.

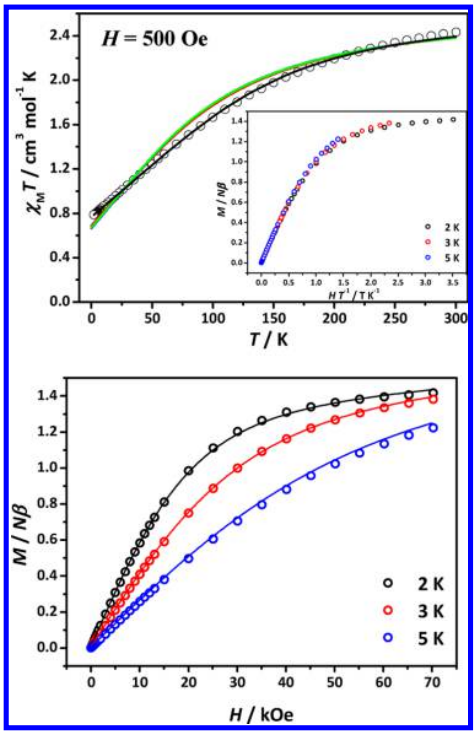

Figure 3. Top: Temperature dependence of the $\chi_M T$ product at 500 Oe. The solid lines are for best fit (black) and ab initio calculations (red, blue, and green), respectively. Inset: molar magnetization ($M/N\beta$) vs H/T at 2.0, 3.0, and 5.0 K, respectively. Bottom: $M/N\beta$ vs magnetic field (H) at 2.0, 3.0, and 5.0 K, respectively. The solid lines are for ab initio calculations.

For assuming the D_{3d} point group, the effective Hamiltonian for the crystal-field perturbations are proposed as:[18a]

$$\hat{H}_{CF} = B_0^2 C_0^2 + B_0^4 C_0^4 + B_3^4 C_3^4 + B_0^6 C_0^6 + B_3^6 C_3^6 + B_6^6 B_6^6$$

The terms containing C_q^k ($q = 3$ and 6) suggest the nonzero of the nondiagonal elements in the crystal-field matrix, leading the terms for which $|M_J - M_J'| = q$ are mixed and are responsible for the fact that M_J will not remain a good quantum number. In order to obtain the electronic structures, we try to fit the static magnetic susceptibility (Figure 3, black solid line) by program CONDON[18b] in the consideration of the spin−orbit coupling, crystal-field (D_{3d}) effect, as well as Zeeman term. The Stark levels of $^2F_{7/2}$ are 0, 230.6, 332.1, and 397.6 cm^{-1} extracting from the fitting result, which are close to the ab initio calculations (vide infra, Table 2). The eigenfunctions of the ground Kramers doublet is the linear combinations involving different $|M_J>$:

$$|KD1> = -0.02|{}^7/_2> - 0.02|-{}^7/_2> + 0.65|{}^5/_2> + 0.67|-{}^5/_2> - 0.26|{}^1/_2> + 0.25|-{}^1/_2>$$

dx.doi.org/10.1021/ic301115b | Inorg. Chem. 2012, 51, 8538−8544

Table 2. Calculated Energies (cm^{-1}) of the Lowest Doublet States Arising from the Atomic Multiplet $J = {}^7/_2$ on Yb^{III} Ion and *g*-Tensor Components of the Ground Doublet State in Different Computational Approximations[a]

A	B	C	D
0.0	0.0	0.0	0.000
163.7	156.9	157.4	187.935
349.4	354.8	356.7	300.026
542.6	547.2	550.9	485.034
main values of the *g*-tensor of the ground doublet			
$g_X = 3.7633$	$g_X = 3.5538$	$g_X = 3.5994$	$g_X = 3.2098$
$g_Y = 2.7126$	$g_Y = 2.8980$	$g_Y = 2.8842$	$g_Y = 2.6944$
$g_Z = 0.7223$	$g_Z = 0.4802$	$g_Z = 0.4491$	$g_Z = 1.7634$

[a]See Supporting Information for details.

$$|KD2> = +0.02|{}^7/_2> - 0.02|-{}^7/_2> + 0.65|{}^5/_2> - 0.67|-{}^5/_2> + 0.26|{}^1/_2> + 0.25|-{}^1/_2>$$

Ab initio calculations performed on the molecular structure (see Supporting Information for details) reveal the following aspects: (a) the ground Kramers doublet state is well separated from the first excited state; (b) if the complex belongs to the phenol type, the *g*-tensor in all doublets are of easy-plane type, which is the result of a high local symmetry of the Yb^{III} ion, being closer to trigonally distorted octahedral than to axial. A perfect reproduction of $M(H)$ dependencies in Figure 3 testifies about an accurate description of the ground Kramers doublet. In comparison, we calculated another situation where the complex belongs to the secondary ammonium type (Table S3, Supporting Information); thus, it is of easy-axis anisotropy. However, both the IR spectrum and pK_a considerations suggest that it should be the former, the phenol type, and the micro-SQUIDS measurement further confirms the complexes are of easy-plane anisotropy, which is the first reported pure lanthanide SMM of this type.

In the absence of dc field, the complex shows no out-of-phase signals of ac magnetic susceptibilities χ_M'' above 1.8 K with the frequency ν = 1 and 1488 Hz (Figure S2, Supporting Information). This result indicates that the magnetization relaxation time (τ) is much shorter than $1/2\pi\nu$. There is no surprise that the quantum tunneling of magnetization (QTM) plays an important role due to the mixture of different $|M_J>$ (see the eigenfunction). When applying a number of dc fields in the wide range of 200−2000 Oe at 1.9 K, a clear slow relaxation process is observed (Figure 4), which may be due to the suppression of QTM,[9d,12a,b] and a maximum of the relaxation time appears at an applied field around 400 Oe.

A set of frequency-dependent out-of-phase signals is observed under a 400 Oe dc field (Figure 5). On cooling, χ_M' increases again below 2.5 K, and this indicates the onset of QTM, as commonly observed in other lanthanide SMMs.[4,7a,8a,b] The ac susceptibilities, along with Cole−Cole plots showing quasi-semicircles and fitted by the generalized Debye function (Figure 6; α = 0.024−0.057),[19] indicate the presence of a very narrow distribution of slow relaxation.

The spin−lattice relaxation time is formulated as: $\tau^{-1} = AT + BT^n + C\exp(-\Delta/k_BT)$.[4b,13,17c−f] The three terms respectively refer to the direct, the Raman, and the Orbach process. In general, n = 7 for non-Kramers ions and n = 9 for Kramers ions, but when optical and acoustic phonons are taken into consideration depending on the structure of energy levels, n = 1−6 is reasonable.[17e,f] We find that the relaxation time obeys the T^{-n} (n = 2.37(4)) behavior instead of an exponential temperature-dependence (Figure 7), suggesting that a superpositive admixture of two types of spin−lattice interaction mechanisms, the single-phonon direct process and optical acoustic Raman-like process, are dominant. We tentatively try the Arrhenius law in the high-temperature range only, extracting the "barrier height" of Δ = 4.9(1) cm^{-1} with the pre-exponential factor $\tau_0 = 2.0 \times 10^{-5}$ s. However, the calculated energies of excited Kramers doublets (Table 1) are 2 orders of magnitude larger than that; therefore, the observed relaxation cannot be of the thermally activated type. To strengthen this conclusion, we show in Figures S8 and S9 (Supporting Information) that if the first excited state was at 4.9 cm^{-1}, then the calculated magnetism would completely not agree with the measured one, further excluding the presence of an Orbach process.

Due to the large contributions of the transversal *g* components, g_X and g_Y, of the ground doublet state (Table 1), in the absence of external magnetic field, the magnetization will not be blocked. Indeed, the large matrix elements of transversal magnetic moments will induce large transversal Zeeman interaction which will efficiently connect strongly a magnetized ground state with the state of opposite magnetization. In such a situation, the blocking of magnetization is only possible under the applied strong dc field which induces a bias between the two states of the Kramers doublet exciting the

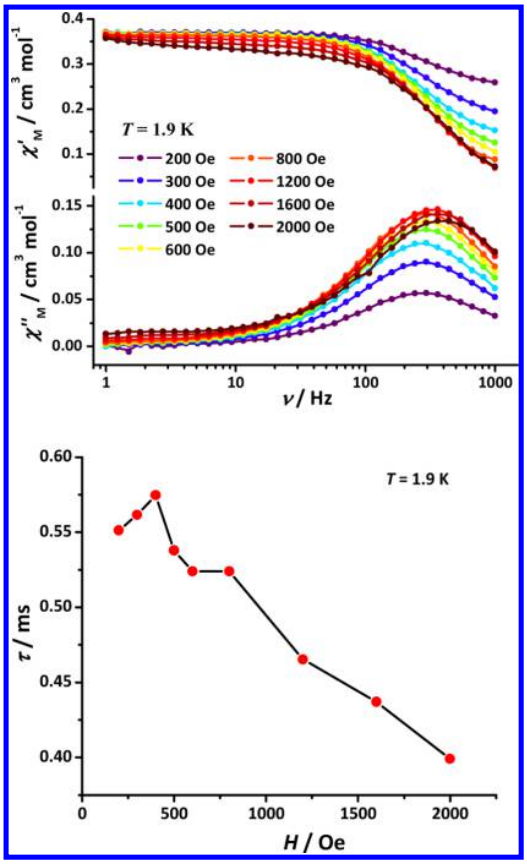

Figure 4. Top: Plot of ac susceptibility vs frequency oscillating at 1−1000 Hz at the indicated applied fields at 1.9 K; bottom: dc field dependence of the relaxation time at 1.9 K. The solid line is a guide for the eye.

dx.doi.org/10.1021/ic301115b | Inorg. Chem. 2012, 51, 8538−8544

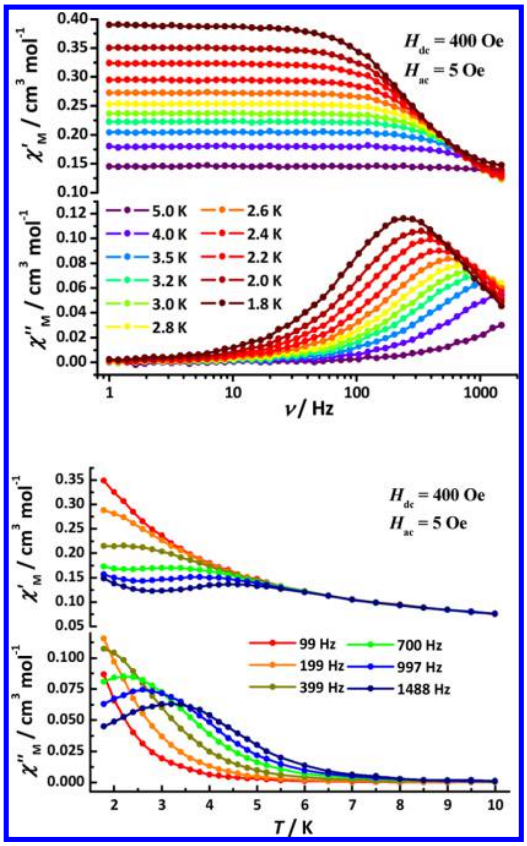

Figure 5. Top: plot of ac susceptibility (in-phase χ_M' and out-of-phase χ_M'' susceptibilities) vs frequency (ν) oscillating at 1−1500 Hz at H_{ac} = 5 Oe and H_{dc} = 400 Oe in the temperature range of 1.8−20 K. Bottom: plot of ac susceptibility vs temperature oscillating at 99−1488 Hz at H_{ac} = 5 Oe and H_{dc} = 400 Oe. The solid line is a guide for the eye.

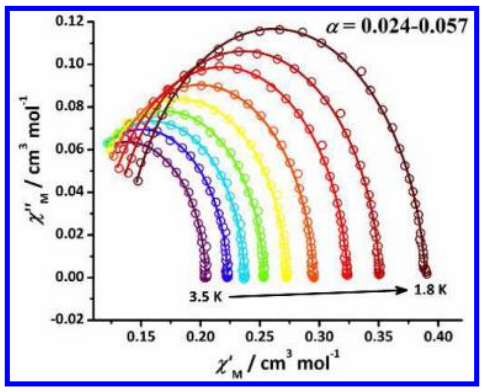

Figure 6. Cole−Cole plot in the temperature range of 3.5−1.8 K. The solid lines represent the best fitting of the experimental data to a generalized Debye model providing α = 0.024−0.057.

Zeeman splitting arising from transversal fields.[1b] Then, increasing the bias by applying stronger dc fields will lead to a stronger localization of the two wave functions corresponding to opposite magnetizations[1b] and, as a result, to a suppression of QTM and an increase of relaxation time. This is accompanied by a single-phonon direct process,[13] whose rate increases fast with the field and finally makes the relaxation time decrease again starting with some value of H_{dc}. This is

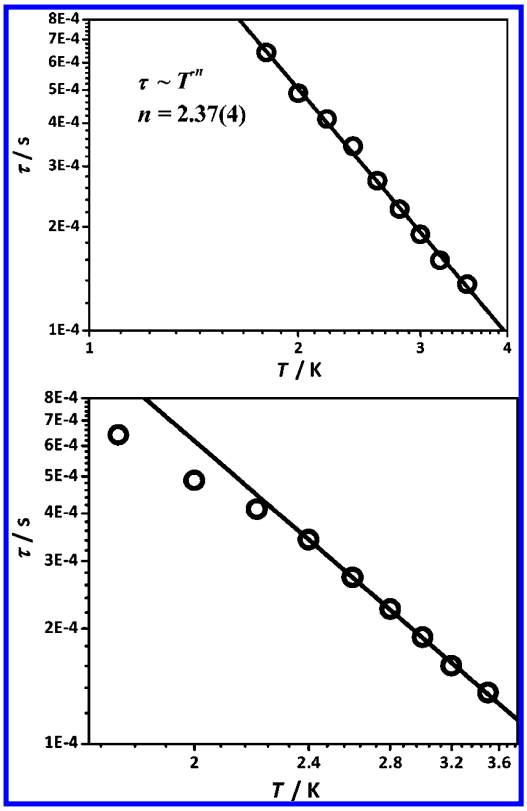

Figure 7. The plot of the relaxation time τ vs T on a log−log scale (top) and a log-reciprocal scale (bottom). The solid lines correspond to the apparent linear fitting. See the text for details.

precisely what is observed in the present complex: τ rises with H_{dc} until the latter reaches the value of 400 Oe and then starts to decrease (Figure 4).

The major difference of the present complex from axial[4,7] and low-symmetric lanthanide complexes and fragments[20] is a much less pronounced axial character of the crystal field surrounding the Yb^{III} ion. Indeed, despite the pseudo S_6 (or pseudo D_{3d}) geometry of its environment (Figure 1 and S1), the crystal field basically looks like a trigonally distorted octahedron. The eigenfunctions of the latter are far from being pure $|J\ M_J>$ but rather are their linear combinations involving strongly differing values of M_J, often of opposite signs. This is confirmed by the g-factors in Tables 1 and S2, which are much lower than g = 8 for Yb^{III} for an effective spin of $^1/_2$. Such a strong admixture of different M_J in the ground Kramers doublet explains the large transversal g-factors in Table 1.

In order to study the magnetic anisotropy, low-temperature single-crystal magnetization measurements were carried out on a micro-SQUID magnetometer.[21a] Using a transverse field method at different angles of the applied field, we could confirm an easy-plane like anisotropy.[21b] Applying the field in the easy plane, a butterfly shaped hysteresis cycle was observed (Figure 8). The strong dependence of hysteresis loops on the field sweep rate and temperature are in accord with the observed field-dependent peaks in ac susceptibility.

■ CONCLUSION

In this study, we have synthesized and fully characterized a 6-coordinate Yb^{III}-based molecule showing field-induced blockage of magnetization. It is showed that the relaxation process is

dx.doi.org/10.1021/ic301115b | Inorg. Chem. 2012, 51, 8538−8544

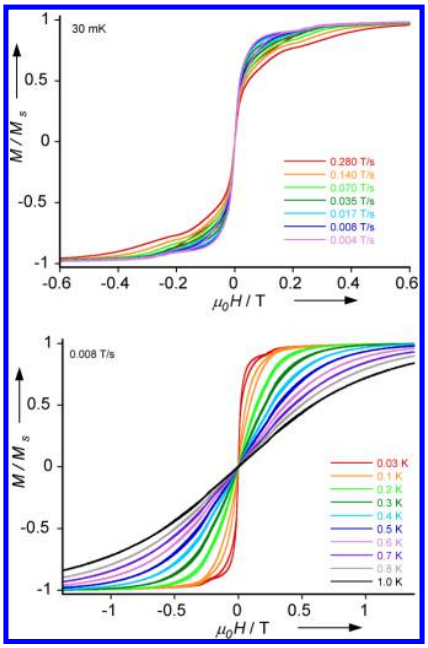

Figure 8. The normalized magnetization (M/Ms) vs applied dc field sweeps at the indicated sweep rate and temperatures, applying the magnetic fields in the easy plane.

assigned to be involved in a direct process and excludes an Orbach process. The coordination sphere of Yb^{III} ion is close to S_6 or D_{3d} local symmetry, leading to easy-plane anisotropy while the investigated complex is the first lanthanide field-induced SMM of this type.

■ ASSOCIATED CONTENT

Supporting Information

Figure S1, structure of the $[Yb^{III}(H_3L)_2]^{3+}$ cation and the coordination environment of Yb^{III}; Figure S2, plot of ac susceptibility vs temperature in a zero dc field; Figure S3, powder X-ray diffraction pattern; ab initio calculations of electronic and magnetic properties of the Yb complex and related figures and tables for the calculations; CIF file. This material is available free of charge via the Internet at http://pubs.acs.org.

■ AUTHOR INFORMATION

Corresponding Author

*E-mail: tongml@mail.sysu.edu.cn (M.-L.T.); Liviu.Chibotaru@chem.kuleuven.be (L.F.C.); wolfgang.wernsdorfer@grenoble.cnrs.fr (W.W.).

Author Contributions

‖These authors contributed equally to this work.

Notes

The authors declare no competing financial interest.

■ ACKNOWLEDGMENTS

This work was supported by the NSFC (Grant Nos. 91122032, 90922009, and 21121061) and the "973 Project" (2012CB821704). L.U. is a postdoc of the FWO-Vlaanderen. Financial support from methusalem program at the K. U. Leuven is gratefully acknowledged. W.W. acknowledges the ANR-PNANO project MolNanoSpin No. ANR-08-NANO-002 and the ERC Advanced Grant MolNanoSpin No. 226558.

■ REFERENCES

(1) (a) Leuenberger, M. N.; Loss, D. *Nature* **2001**, *410*, 789. (b) Gatteschi, D.; Sessoli, R.; Villain, J. *Molecular Nanomagnets*; Oxford University Press: New York, 2006. (c) Bogani, L.; Wernsdorfer, W. *Nat. Mater.* **2008**, *7*, 179. (d) Stone, R. *Science* **2009**, *325*, 1336. (e) Dei, A.; Gatteschi, D. *Angew. Chem., Int. Ed.* **2011**, *50*, 11852. (f) Aromí, G.; Aguilà, D.; Gamez, P.; Luis, F.; Roubeau, O. *Chem. Soc. Rev.* **2012**, *41*, 537. (g) Gatteschi, D.; Sessoli, R. *Angew. Chem., Int. Ed.* **2003**, *42*, 268.

(2) (a) Sessoli, R.; Tsai, H.-L.; Schake, A. R.; Wang, S.; Vincent, J. B.; Folting, K.; Gatteschi, D.; Christou, G.; Hendrickson, D. N. *J. Am. Chem. Soc.* **1993**, *115*, 1804. (b) Sessoli, R.; Gatteschi, D.; Caneschi, A.; Novak, M. A. *Nature* **1993**, *365*, 141. (c) Sessoli, R.; Powell, A. K. *Coord. Chem. Rev.* **2009**, *253*, 2328. (d) Wang, B.-W.; Jiang, S.-D.; Wang, X.-T.; Gao, S. *Sci. China Chem.* **2009**, *52*, 1739. (e) Ishikawa, N *Struct. Bonding (Berlin)* **2010**, *135*, 211. (f) Rinehart, J. D.; Long, J. R. *Chem. Sci.* **2011**, *2*, 2078.

(3) (a) Murugesu, M.; Habrych, M.; Wernsdorfer, W.; Abboud, K. A.; Christou, G. *J. Am. Chem. Soc.* **2004**, *126*, 4766. (b) Ako, A. M.; Hewitt, I. J.; Mereacre, V.; Clérac, R.; Wernsdorfer, W.; Anson, C. E.; Powell, A. K. *Angew. Chem., Int. Ed.* **2006**, *45*, 4926. (c) Wang, W.-G.; Zhou, A.-J.; Zhang, W.-X.; Tong, M.-L.; Chen, X.-M.; Nakano, M.; Beedle, C. C.; Hendrickson, D. N. *J. Am. Chem. Soc.* **2007**, *129*, 1014.

(4) (a) Ishikawa, N.; Sugita, M.; Ishikawa, T.; Koshihara, S.-y.; Kaizu, Y. *J. Am. Chem. Soc.* **2003**, *125*, 8694. (b) Ishikawa, N.; Sugita, M.; Ishikawa, T.; Koshihara, S.; Kaizu, Y. *J. Phys. Chem. B* **2004**, *108*, 11265.

(5) (a) Takamatsu, S.; Ishikawa, T.; Koshihara, S.-y.; Ishikawa, N. *Inorg. Chem.* **2007**, *46*, 7250. (b) Ishikawa, N.; Sugita, M.; Wernsdorfer, W. *Angew. Chem., Int. Ed.* **2005**, *44*, 2931. (c) Ishikawa, N.; Sugita, M.; Wernsdorfer, W. *J. Am. Chem. Soc.* **2005**, *127*, 3650. (d) Ishikawa, N.; Sugita, M.; Okubo, T.; Tanaka, N.; Lino, T.; Kaizu, Y. *Inorg. Chem.* **2003**, *42*, 2440.

(6) Branzoli, F.; Carretta, P.; Filibian, M.; Zoppellaro, G.; Graf, M. J.; Galan-Masaros, J. R.; Fuhr, O.; Brink, S.; Ruben, M. *J. Am. Chem. Soc.* **2009**, *131*, 4387.

(7) (a) AlDamen, M. A.; Cardona-Serra, S.; Clemente-Juan, J. M.; Coronado, E.; Gaita-Ariño, A.; Martí-Gastaldo, C.; Luis, F.; Montero, O. *Inorg. Chem.* **2009**, *48*, 3467. (b) AlDamen, M. A.; Clemente-Juan, J. M.; Coronado, E.; Martí-Gastaldo, C.; Gaita-Ariño, A. *J. Am. Chem. Soc.* **2008**, *130*, 8874. (c) Yamashita, A.; Watanabe, A.; Akine, S.; Nabeshima, T.; Nakano, M.; Yamamura, T.; Kajiwara, T. *Angew. Chem., Int. Ed.* **2011**, *50*, 4016. (d) Feltham, H. L. C.; Lan, Y.; Klöwer, F.; Ungur, L.; Chibotaru, L. F.; Powell, A. K.; Brooker, S. *Chem.—Eur. J.* **2011**, *17*, 4362. (e) Feltham, H. L. C.; Klöwer, F.; Cameron, S. A.; Larsen, D. S.; Lan, Y.; Tropiano, M.; Faulkner, S.; Powell, A. K.; Brooker, S. *Dalton Trans.* **2011**, *40*, 11425.

(8) (a) Bi, Y.; Guo, Y.-N.; Zhao, L.; Guo, Y.; Lin, S.-Y.; Jiang, S.-D.; Tang, J.; Wang, B.-W.; Gao, S. *Chem.—Eur. J.* **2011**, *17*, 12476. (b) Jiang, S.-D.; Wang, B.-W.; Su, G.; Wang, Z.-M.; Gao, S. *Angew. Chem., Int. Ed.* **2010**, *49*, 7448. (c) Jiang, S.-D.; Wang, B.-W.; Sun, H.-L.; Wang, Z.-M.; Gao, S. *J. Am. Chem. Soc.* **2011**, *133*, 4730.

(9) (a) Li, D.-P.; Zhang, X.-P.; Wang, T.-W.; Ma, B.-B.; Li, C.-H.; Li, Y.-Z.; You, X.-Z. *Chem. Commun.* **2011**, *47*, 6867. (b) Li, D.-P.; Wang, T.-W.; Li, C.-H.; Liu, D.-S.; Li, Y.-Z.; You, X.-Z. *Chem. Commun.* **2010**, *46*, 2929. (c) Cucinotta, G.; Perfetti, M.; Luzon, J.; Etienne, M.; Car, P.-E.; Caneschi, A.; Calvez, G.; Bernot, K.; Sessoli, R. *Angew. Chem., Int. Ed.* **2012**, *51*, 1606. (d) Sugita, M.; Ishikawa, N.; Ishikawa, T.; Koshihara, S.-y.; Kaizu, Y. *Inorg. Chem.* **2006**, *45*, 1299.

(10) Magnani, N.; Apostolidis, C.; Morgenstern, A.; Colineau, E.; Griveau, C.; Bolvin, H.; Walter, O.; Caciuffo, R. *Angew. Chem., Int. Ed.* **2011**, *50*, 1696.

(11) (a) Rinehart, J. D.; Long, J. R. *J. Am. Chem. Soc.* **2009**, *131*, 12558. (b) Rinehart, J. D.; Meihaus, K. R.; Long, J. R. *J. Am. Chem. Soc.* **2010**, *132*, 7572.

(12) (a) Freedman, D. E.; Harman, W. H.; Harris, T. D.; Long, G. J.; Chang, C. J.; Long, J. R. *J. Am. Chem. Soc.* **2010**, *132*, 1224. (b) Harman, W. H.; Harris, T. D.; Freeman, D. E.; Fong, H.; Chang, A.; Rinehart, J. D.; Ozarowski, A.; Sougrati, M. T.; Grandjean, F.;

Long, G. J.; Long, J. R.; Chang, C. J. *J. Am. Chem. Soc.* **2010**, *132*, 18115. (c) Zadrozny, J. M.; Long, J. R. *J. Am. Chem. Soc.* **2011**, *133*, 20732. (d) Zadrozny, J. M.; Liu, J.; Piro, N. A.; Chang, C. J.; Hill, S.; Long, J. R. *Chem. Commun.* **2012**, *48*, 3927. (e) Jurca, T.; Farghal, A.; Lin, P.-H.; Korobkov, I.; Murugesu, M.; Richeson, D. S. *J. Am. Chem. Soc.* **2011**, *133*, 15814. (f) Lin, P.-H.; Smythe, N. C.; Gorelsky, S. I.; Maguire, S.; Henson, N. J.; Korobkov, I.; Scott, B. L.; Gordon, J. C.; Baker, R. T.; Murugesu, M. *J. Am. Chem. Soc.* **2011**, *133*, 15806. (g) Weismann, D.; Sun, Y.; Lan, Y.; Wolmershauser, G.; Powell, A. K.; Sitzmann, H. *Chem.—Eur. J.* **2011**, *17*, 4700.

(13) Abragam, A.; Bleaney, B. *Electron Paramagnetic Resonance of Transition Ions*; Clarendon Press: Oxford, 1970.

(14) (a) Liu, S.; Yang, L.-W.; Rettig, S.; Orvig, C. *Inorg. Chem.* **1993**, *32*, 2773. (b) Rived, F.; Rosés, M.; Bosch, E. *Anal. Chim. Acta* **1998**, *374*, 309.

(15) (a) van der Sluis, P.; Spek, A. L. *Acta Crystallogr.* **1990**, *A46*, 194. (b) Sheldrick, G. M. *Acta Crystallogr.* **2008**, *A64*, 112.

(16) Σ is defined as the sum of the absolute values of the deviation from 90° of the 12 *cis* angles in the coordination sphere. See: (a) Alvarez, S.; Alemany, P.; Casanova, D.; Cirera, J.; Llunell, M.; Avnir, D. *Coord. Chem. Rev.* **2005**, *249*, 1693. (b) Alvarez, S.; Avnir, D.; Llunell, M.; Pinsky, M. *New J. Chem.* **2002**, *26*, 996. (c) Guionneau, P.; Brigouleix, C.; Barrans, Y.; Goeta, A. E.; Létrad, J.-F.; Howard, J. A. K.; Gaultier, J.; Chasseau. *D. C. R. Acad. Sci., Ser. IIc: Chim.* **2001**, *4*, 161. (d) Guionneau, P.; Marchivie, M.; Bravic, G.; Létard, J.-F.; Chasseau, D. *J. Mater. Chem.* **2002**, *12*, 2546.

(17) (a) Kahn, O. *Molecular Magnetism*; VCH Publishers: New York, 1993. (b) Miller, J. S.; Drillon, M. *Magnetism: Molecules to Materials*; Weinheim: Wiley-VCH, 2005; Vol *V*. (c) Carlin, R. L. *Magnetochemistry*; Springer-Verlag: New York, 1986. (d) Carlin, R. L.; van Duyneveldt, A. J. *Magnetic Properties of Transition Metal Compounds*; Springer-Verlag: New York, 1977. (e) Singh, A.; Shrivastava, K. N. *Phys. Status Solidi B* **1979**, *95*, 273. (f) Shrivastava, K. N. *Phys. Status Solidi B* **1983**, *117*, 437.

(18) (a) Görller-Walrand, C.; Binnemans, K. Rationalization of Crystal-Field Parameterization. In *Handbook on the Physics and Chemistry of Rare Earths*; Gschneidner, K. A., Jr., Eyring, L., Eds.; Elsevier: Amsterdam, 1996; Vol. *23*, p 121. (b) Schilder, H.; Lueken, H. *J. Magn. Magn. Mater.* **2004**, *281*, 17.

(19) Cole, K. S.; Cole, R. H. *J. Chem. Phys.* **1941**, *9*, 34.

(20) (a) Chibotaru, L. F.; Ungur, L.; Soncini, A. *Angew. Chem., Int. Ed.* **2008**, *47*, 4126. (b) Guo, Y.-N.; Xu, G.-F.; Wernsdorfer, W.; Ungur, L.; Guo, Y.; Tang, J.; Zhang, H.-J.; Chibotaru, L. F.; Powell, A. K. *J. Am. Chem. Soc.* **2011**, *133*, 11948. (c) Ungur, L.; Chibotaru, L. F. *Phys. Chem. Chem. Phys.* **2011**, *13*, 20086. (d) Liu, J.-L.; Guo, F.-S.; Meng, Z.-S.; Zheng, Y.-Z.; Leng, J.-D.; Tong, M.-L.; Ungur, L.; Chibotaru, L. F.; Heroux, K. J.; Hendrickson, D. N. *Chem. Sci.* **2011**, *2*, 1268.

(21) (a) Wernsdorfer, W *Adv. Chem. Phys.* **2001**, *118*, 99. (b) Wernsdorfer, W.; Chakov, N. E.; Christou, G. *Phys. Rev. B* **2004**, *70*, 132413.